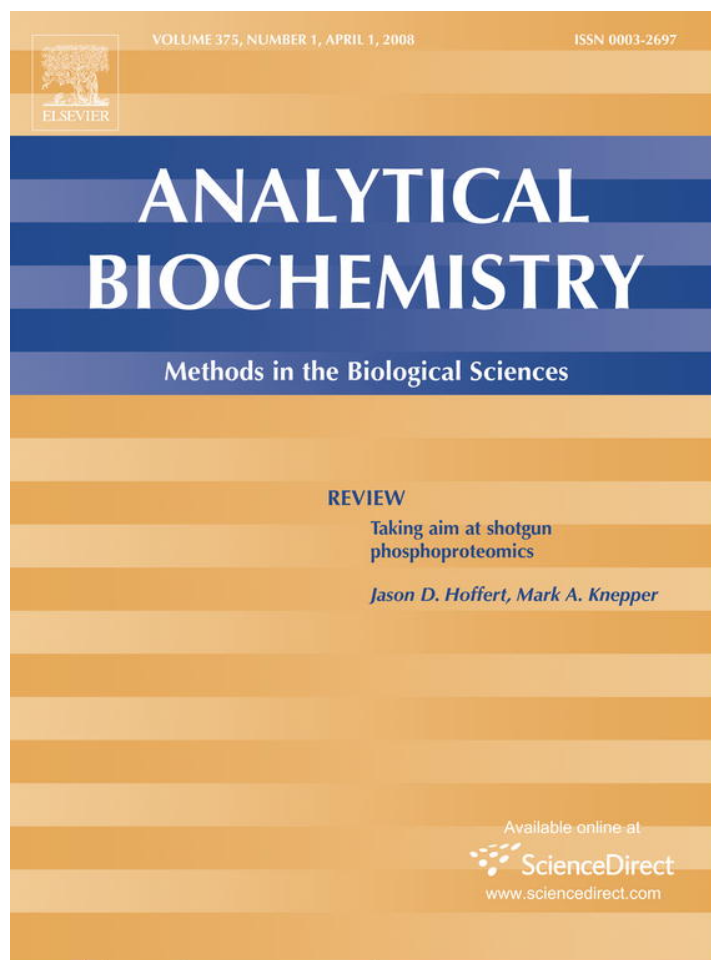


Provided for non-commercial research and education use.
Not for reproduction, distribution or commercial use.



This article was published in an Elsevier journal. The attached copy is furnished to the author for non-commercial research and education use, including for instruction at the author's institution, sharing with colleagues and providing to institution administration.

Other uses, including reproduction and distribution, or selling or licensing copies, or posting to personal, institutional or third party websites are prohibited.

In most cases authors are permitted to post their version of the article (e.g. in Word or Tex form) to their personal website or institutional repository. Authors requiring further information regarding Elsevier's archiving and manuscript policies are encouraged to visit:

<http://www.elsevier.com/copyright>



Dual-fluorophore quantitative high-throughput screen for inhibitors of BRCT–phosphoprotein interaction

Anton Simeonov^a, Adam Yasgar^a, Ajit Jadhav^a, G.L. Lokesh^b, Carleen Klumpp^a,
Sam Michael^a, Christopher P. Austin^a, Amarnath Natarajan^{b,*}, James Inglese^{a,*}

^a NIH Chemical Genomics Center, National Human Genome Research Institute, National Institutes of Health, Bethesda, MD 20892, USA

^b Chemical Biology Program, Department of Pharmacology and Toxicology, University of Texas Medical Branch, Galveston, TX 77555, USA

Received 16 October 2007

Available online 5 December 2007

Abstract

Finding specific small-molecule inhibitors of protein–protein interactions remains a significant challenge. Recently, attention has grown toward “hot spot” interactions where binding is dominated by a limited number of amino acid contacts, theoretically offering an increased opportunity for disruption by small molecules. Inhibitors of the interaction between BRCT (the C-terminal portion of BRCA1, a key tumor suppressor protein with various functions) and phosphorylated proteins (Abraxas/BACH1/CtIP), implicated in DNA damage response and repair pathways, should prove to be useful in studying BRCA1’s role in cancer and in potentially sensitizing tumors to chemotherapeutic agents. We developed and miniaturized to a 1536-well format and 3- μ l final volume a pair of fluorescence polarization (FP) assays using fluorescein- and rhodamine-labeled pBACH1 fragment. To minimize the effect of fluorescence artifacts and to increase the overall robustness of the screen, the 75,552 compound library members all were assayed against both the fluorescein- and rhodamine-labeled probe–protein complexes in separate but interleaved reactions. In addition, every library compound was tested over a range of concentrations following the quantitative high-throughput screening (qHTS) paradigm. Analyses of the screening results led to the selection and subsequent confirmation of 16 compounds active in both assays. Faced with a traditionally difficult protein–protein interaction assay, by performing two-fluorophore qHTS, we were able to confidently select a number of actives for further studies. © 2007 Elsevier Inc. All rights reserved.

Keywords: Quantitative high-throughput screening; BRCT; pBACH1; Fluorescence polarization assay; Hotspot interaction; 1536-Well plate

Protein–protein interactions (PPIs)¹ mediate a myriad of critical cellular processes and, therefore, have grown in prominence recently as targets for drug development. Unlike enzyme active sites, which often are well characterized and of limited size and complexity, the interfaces involved in PPIs often are large and ill defined and may include variable contact points [1]. Such fluid topologies

reflect the lower affinity and transient nature of these interactions and their roles in triggering a variety of signaling events in response to subtle changes in the concentrations and ratios of multiple binding partners. It is not surprising, therefore, that such large and variable interaction space presents enormous challenges to those wishing to identify small molecules that disrupt these interactions in a potent, specific, and reproducible manner. Present-day screening compound libraries, although generally suitable for finding effectors for “druggable” targets such as enzymes and receptors, might not contain the chemotypes needed to disrupt PPIs [2]. In addition to the expansiveness and low definition of the interacting protein surfaces, technical issues pertaining to assay design and screening artifacts further complicate the identification of true PPI disrupters [3].

* Corresponding authors.

E-mail addresses: amnatara@utmb.edu (A. Natarajan), jinglese@mail.nih.gov (J. Inglese).

¹ Abbreviations used: PPI, protein–protein interaction; qHTS, quantitative high-throughput screening; FP, fluorescence polarization; DTT, dithiothreitol; DMSO, dimethyl sulfoxide; FITC, fluorescein isothiocyanate; TAMRA, 5-carboxytetramethyl rhodamine; FRD, Flying Reagent Dispenser; MSR, minimum significant ratio.

For example, colloidal aggregates spontaneously formed by certain compounds might reach the size and topology sufficient to perturb PPIs in a reproducible yet nonspecific and biologically irrelevant manner [2,4,5].

It has been noted recently that in a number of PPI systems, the major contribution to the change in free energy is from a limited number of amino acid contacts. These contacts are commonly referred to as “hot spots,” and currently targeting them for disruption by small molecules is considered to offer improved chances of inhibitor identification [6,7]. Hot spot interactions appear to be better defined and are operationally easier to study because limited-length peptides frequently can be designed to mimic at least one of the interacting partners. In the current study, we focused on the hot spot interaction between the C-terminal domain of BRCA1 and phosphorylated proteins (Abraxas/BACH1/CtIP) [8–11]. These BRCA1–phosphoprotein interactions have been implicated in a variety of cellular functions (e.g., cell cycle regulation, transcription activation/repression and ubiquitination) that are critical for the DNA damage response and repair signaling pathways [9,10,12–17].

Structural and biochemical studies between BRCT (the C-terminal portion of BRCA1) and phosphorylated peptides have led to the identification of a pSXXF as the binding motif on the peptide and mapped the binding site to a region at the interface of the two BRCT domains of BRCA1 [12,14,18–24]. The BRCT–phosphoprotein interactions are transient, and structural studies show that BACH1 and CtIP bind to the same site on the BRCT domains. This strongly suggests the need for temporal regulation of the BRCT–phosphoprotein interactions for the proper functioning of the DNA damage response and repair pathways. Therefore, classical biochemical techniques have limited ability to dissect these signaling pathways, and small molecules are emerging as a viable alternative. Small molecule inhibitors of the BRCT–phosphoprotein interactions should prove to be useful as chemical probes to uncouple the complex BRCA1 signaling and as potential compounds that can be developed as leads to sensitize tumors to DNA damage-based chemotherapeutic agents.

In this work, we describe the development and quantitative high-throughput screening (qHTS) of a BRCT–phosphopeptide interaction assay. Inhibitors of BRCT–phosphopeptide binding were detected by a decrease in the fluorescence polarization (FP) of the fluorophore in a fluorescently labeled phosphorylated 10-amino-acid peptide fragment of BACH1 complexed with BRCT. To minimize the effect of fluorescence artifacts and to increase the overall robustness of the screen, the compound library members were assayed in separate reactions with fluorescein- and rhodamine-labeled probe–protein complexes. In addition, each compound was tested at a minimum of seven concentrations following our previously reported qHTS paradigm [25]. Here we describe the development of a red-shifted FP probe, the miniaturization of fluores-

cein- and rhodamine-based assays to a 3- μ l volume in a 1536-well format, the results of screening both assays across a more than 75,000-compound collection, and the preliminary characterization of actives identified.

Materials and methods

Reagents

Tween 20, EDTA, NaCl, NaN₃, and dithiothreitol (DTT) were procured from Sigma–Aldrich. Dimethyl sulfoxide (DMSO, certified ACS grade) was obtained from Fisher. Unlabeled control peptide SRSTpSPTFNK was synthesized and HPLC purified by the Tufts University Core Facility. The screening assay was performed in 20 mM phosphate buffer (pH 7.3) containing 150 mM NaCl, 1 mM DTT, 1 mM EDTA, 0.02% NaN₃, and 0.01% Tween 20. Fluorescein- and rhodamine-labeled peptides were prepared via standard coupling methods. HPLC-purified to 95% purity, and analyzed by LC-MS to ensure the incorporation of single fluorophore per peptide.

Compound library

The 75,552-member library was composed of two main subsets: 60,783 compounds from the NIH Molecular Libraries Small Molecule Repository (<http://www.mli.nih.gov>), prepared as 10-mM stock solutions in 384-well plates and delivered by Galapagos Biofocus DPI (South San Francisco, CA, USA, <http://mlsmr.glp.com>), and an NCGC internal exploratory collection of 11,336 compounds that consisted of several commercially available libraries of known bioactives: 1280 compounds from Sigma–Aldrich (LOPAC1280 library), 1120 compounds from Prestwick Chemical (Washington, DC, USA), 980 compounds from Tocris (Ellisville, MO, USA), 280 purified natural products from TimTec (Newark, DE, USA), 1980 compounds from the National Cancer Institute (NCI Diversity Set), and collections from other commercial and academic collaborators (three 1000-member combinatorial libraries from Pharmacopeia [Cranbury, NJ, USA], 1121 compounds from the Boston University Center for Chemical Methodology and Library Development, a 96-member peptide library from Sam Gelman’s laboratory [University of Wisconsin–Madison], and 991 compounds from the University of Pittsburgh Center for Chemical Methodology and Library Development). The compound library (7 μ l each in 1536-well Greiner polypropylene compound plates) was prepared as DMSO solutions at initial concentrations ranging between 2 and 10 mM. Plate-to-plate (vertical) dilutions and 384-to-1536 compressions were performed on an Evolution P3 dispense system equipped with a 384-tip pipetting head and two RapidStak units (PerkinElmer, Wellesley, MA, USA). Additional details on the preparation of the compound library were provided by Ingles and coworkers [25].

Control plate

Titration of the unlabeled decapeptide SRSTpSPTFNK was delivered via pin transfer of 23 nl of solution per well from a separate source plate to the upper half of column 2 of each assay plate. The starting concentration of the control was 10 mM, followed by twofold dilution points in duplicate, for a total of eight concentrations, resulting in a final assay concentration range from 76 to 0.59 μ M, corresponding to the dilution of 23 nl into 3 μ l.

qHTS protocol with assay interleaving

As shown in Table 1, 3 μ l of reagents (100 nM fluorescein isothiocyanate [FITC]- or 5-carboxytetramethyl rhodamine [TAMRA]-labeled peptide in columns 3 and 4 as negative control and 100 nM labeled peptide and BRCT [100 nM in the TAMRA assay and 250 nM in the FITC assay] mixture in columns 1, 2, and 5–48) was dispensed to a 1536-well Greiner black assay plate. Compounds and control (23 nl) were transferred via a pin tool (Kalypsys, San Diego, CA, USA) equipped with a 1536-pin array (10 nl slotted pins, V&P Scientific, San Diego, CA, USA) [26]. The plate was incubated for 12 min at room temperature and then read on a ViewLux high-throughput CCD imager (PerkinElmer) using FITC polarization filter sets for the fluorescein-based assay and BODIPY sets for the rhodamine-based assay. During dispense, reagent bottles were kept submerged in a 4 °C recirculating chiller bath, and all liquid lines were covered with aluminum foil to minimize probe and protein degradation. All screening operations were performed on a fully integrated robotic

system (Kalypsys) containing one RX-130 and two RX-90 anthropomorphic robotic arms (Staubli, Duncan, SC, USA). Library plates were screened starting from the lowest concentration and proceeding to the highest one. The timing and order of assay plates passing through the screening system were adjusted such that each compound library plate was assayed against the fluorescein- and rhodamine-labeled assay systems at immediately adjacent time points. Vehicle-only plates, with DMSO being pin transferred to the entire columns 5–48 compound area, were included at uniform intervals of approximately every 50 plates to record any systematic shifts in assay signal.

Analysis of qHTS data

Screening data were corrected and normalized and concentration–effect relationships were derived by using algorithms developed in-house. Percentage activity was computed from the median values of the uninhibited (or neutral) control (48 wells located in column 1 and one-half of column 2) and the free probe (or 100% inhibited) control (64 wells located in entire columns 3 and 4). For assignment of plate concentrations and sample identifiers, ActivityBase (ID Business Solutions, Guildford, UK) was used for compound and plate registrations. An in-house database was used to track sample concentrations across plates. Plates containing DMSO only (instead of compound solutions) were inserted uniformly throughout the screen to monitor any systematic trend in the assay signal potentially resulting from issues with reagent dispensers or a decrease in enzyme-specific activity. Correction factors were generated from the DMSO plate data and applied to each assay plate to correct for such systematic errors. A four-parameter Hill equation [27] was fitted to the concentration–response data by minimizing the residual error between the modeled and observed responses. Outliers could be identified and masked by modeling the Hill equation and asking whether the difference exceeded that expected from the noise in the assay.

Follow-up testing of primary screen actives

Screening actives selected for follow-up testing were obtained as 10-mM initial stock solutions in DMSO. The samples were then serially diluted row-wise in 384-well plates in twofold steps for a total of 12 concentrations ranging from 10 mM to 4.9 μ M. On completion of the 12-point dilution, solutions from two 384-well plates were transferred to duplicate wells of a 1536-well compound plate. The last two rows of the 1536-well plate did not contain any test compound and were reserved for placement of positive and negative controls. The assay protocol for confirmation was essentially the same as that described above for the qHTS protocol. A Flying Reagent Dispenser (FRD, Aurora Discovery, currently Beckman–Coulter) [28] was used to dispense reagents into the assay plates. Pin transfer of 23 nl of compound solution into 3 μ l of assay mixture

Table 1
BRCA1 interleaved qHTS protocol

Step	Parameter	Value	Description
1	Reagent	3 μ l	Complex and free probe solutions
2	Library compounds	23 nl	76 μ M to 0.97 nM titration series
3	Controls	23 nl	Decapeptide titration intraplate
4	Time, speed	15 s, 200 \times g	Centrifugation
5	Incubation time	12 min	Compound interaction with targets
6	Assay readout	Ex 480/Em 540 nm and Ex 525/Em 598 nm	ViewLux fluorescence polarization read

Step notes

- 1 Black solid-bottom plates, single-tip dispense, green/red complex in columns 1, 2, and 5–48, green/red free probe in columns 3 and 4
- 2 Pin tool transfer of library into columns 5–48
- 3 Pin tool transfer of decapeptide SRSTpSPTFNK titration into upper half of column 2
- 4 Plate centrifugation to remove bubbles
- 5 Room temperature incubation in auxiliary hotel
- 6 FP as well as parallel and perpendicular light intensity values collected

resulted in final compound concentrations between 76 μM and 37 nM.

Results

Assay principle, miniaturization, and optimization

The assay initially was developed and optimized in a 384-well format by following the FP change in the fluorescein label (hereafter referred to as “green”) [29]. During these studies, the main parameters of the assay, such as buffer conditions, concentrations of probe and protein, and DMSO and detergent tolerance, were tested and optimized. The assay was miniaturized to a final volume of 3 μl in a 1536-well format by direct volume reduction. In addition, to prevent peptide and protein adsorption to the polystyrene wells due to the increased surface-to-volume ratio, and to minimize the interfering effect of promiscuous inhibitors acting via colloidal aggregate formation [4,5], we included detergent (0.01% Tween 20) in the assay buffer.

In parallel with the miniaturization of the original green assay, a red-shifted probe was explored. We wanted to screen the current system against the two differently labeled protein–phosphopeptide complexes so as to increase the confidence in the actives found and possibly to maximize the chances of identifying actives. Thus, a pBACH1 peptide of the same sequence was labeled with TAMRA (hereafter referred to as “red”) and subjected to the same assay optimization experiments. The FP dynamic range observed with the red-labeled peptide was higher, in the range of 170 to 190 mP, as is frequently experienced with this fluorophore, while in a control experiment, protein addition to free rhodamine dye did not result in FP change (not shown). Due to the increased FP change afforded by the red label per equivalent protein concentration, the latter was decreased to 100 nM, the same as that of the labeled probe, thereby resulting in reagent savings and improving the response range of the assay (data not shown). All four major assay components (green and red free probes and protein complexes) were tested and found to be stable for at least 24 h when formulated as stock solution at their working concentrations (Fig. 1). Such demonstrated stability permitted the implementation of an unattended overnight screening experiment.

Interleaved dual-assay qHTS

Given that both assay reagents and compounds in the screening collection may exhibit temporal variations in activity [30,31], we optimized the screening protocol to test each compound sample in the two individual fluorophore assays as closely in time as possible. There was no specific way within the robotic software to ensure that assay plates were run in an alternating fashion between the green and red systems or to set up any explicit dependencies or contingencies between the two assays. Because the same pin tool and plate reader were used for both assays, the only

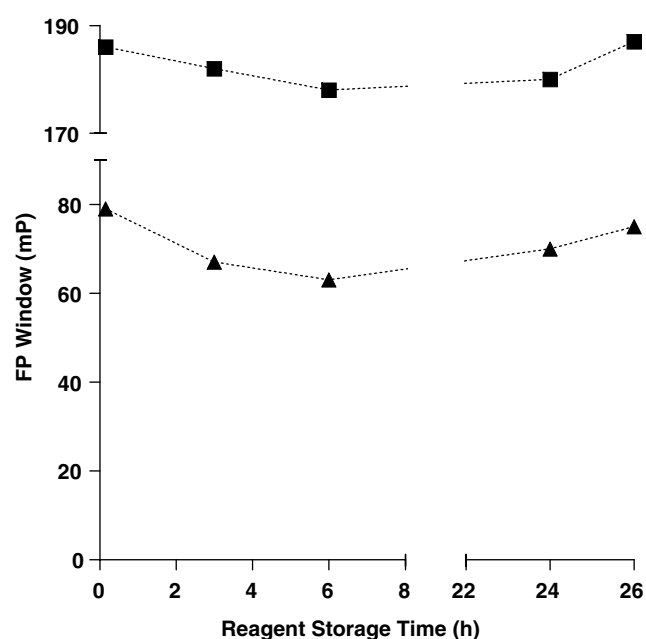


Fig. 1. Screening reagents' stability as a function of storage time. Bottles containing complex and free probe stock solutions were prepared and kept at 4 °C. At the selected time points, the bottles were connected to a liquid dispenser and the assay was performed as described in Materials and Methods. FP signal windows (solid triangles for green assay and solid squares for red assay) were computed as the average of 32 wells.

option remaining was to interleave plates from the two assays based on time. We achieved this by adding an incubation step to only one of the two assay methods (robotic protocols), thereby staggering the start times of the two assays and successfully achieving alternation of the two colors. Fig. 2 represents a schematic of the fluorophore interleaving strategy to ensure testing of each library plate against green and red fluorescent complexes at adjacent time points.

Implementation of this innovative robotic protocol required addressing two potential bottlenecks. First, to prevent competition between the methods for the pin transfer station, the offset was applied to the second method only so that when the two methods were interleaved they would be evenly spaced due to the offset applied to the second method. Second, because the robot arms were also shared between the methods, competition for them eventually could lead to enough mistiming of one or both methods that they no longer would be cleanly cyclically interleaved. To prevent this, we added six assay plates to the end of each fluorophore screen into which DMSO, rather than test compounds, was pin transferred. This technique is conceptually similar to time domain-based interpolation used in digital signal processing methods and sometimes is referred to as a “zero pad,” where a string of zeros is applied to the end of a time domain sequence to increase the resolution of the frequency domain sampling. In our case, the “zeros” used were the blank DMSO plates at the end of the screen, and the time domain sequence was the series of steps that each assay plate goes

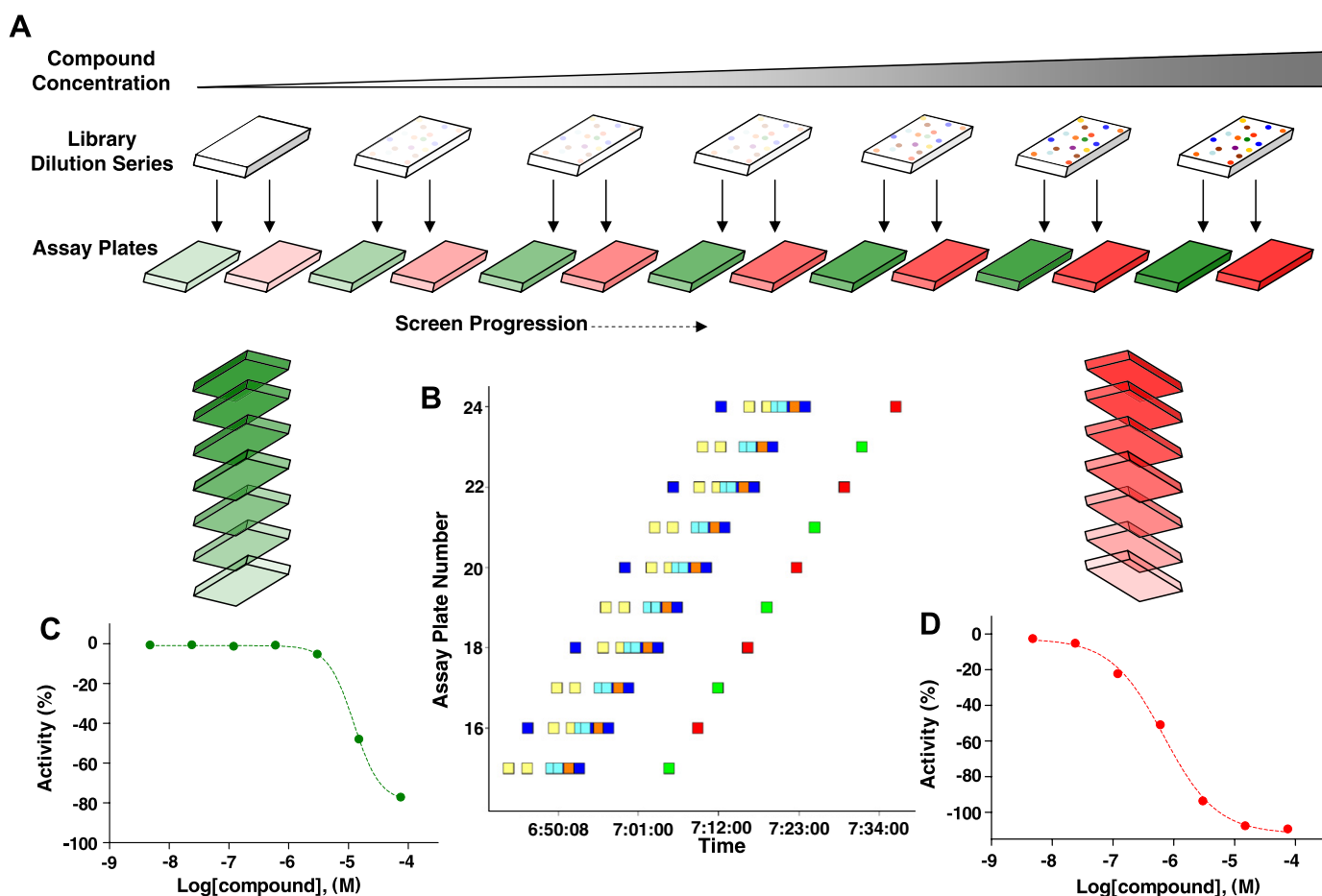


Fig. 2. Interleaving of dual-fluorophore screens. From each compound library plate, samples were pin transferred into green and red fluorophore assay plates in immediate succession. Shown are the schematic representation of interleaving (A) along with examples of assay plates passing through the screening system (Spotfire plot in panel B) and concentration–response curves derived from the green screening assay (C) and red screening assay (D). The plots are color coded to reflect the assay fluorophore.

through during the screen. By adding these blank plates, we maintained the system steady state and thereby allowed all compound plates to be screened in a consistently interleaved fashion, spaced approximately 3 minutes apart.

qHTS performance and analysis

The screens against the green- and red-labeled systems used 470 and 473 assay plates, respectively, and all 943 plates were run interleaved in one uninterrupted robotic screening run (Fig. 2). The assay signal windows, as expressed by the difference between mean FP values for the bound and unbound labeled peptide controls, were stable throughout the screen (Fig. 3A). Both assays performed robustly, yielding average Z' factors [32] of 0.84 and 0.91 for the green and red assay systems, respectively (Fig. 3B). The intraplate decapeptide control titration curves remained nearly overlapping throughout the screen progression (Fig. 3C), resulting in average IC_{50} values of 4.2 and 5.0 μ M for the green and red systems, respectively. During this qHTS experiment, the library members were tested in a concentration–response of at least seven points, with concentrations ranging from 0.97 nM to 76 μ M, and

for each well and assay system, FP as well as parallel and perpendicular plane fluorescence intensity values were collected and stored in the database.

Unlike traditional HTS, qHTS provides concentration–responses for all of the compounds screened and allows determination of an AC_{50} value, defined as the half-maximal activity concentration, for each compound in the primary screen. Concentration–response curves were assigned to one of four classes based on efficacy (response magnitude), presence of asymptotes, and goodness of fit of the curve to the data (r^2) [25]. For the current screen, the activity associated with each well was computed from the FP values normalized against control wells. In addition, the fluorescence intensity values associated with each well were stored in the database and used to further scrutinize purported actives.

Overview of actives

The green and red screens yielded a total of 47 active samples associated with varying quality concentration–response curves. Of the 47 samples, 2 represented duplicates, being the same compound that existed in the collec-

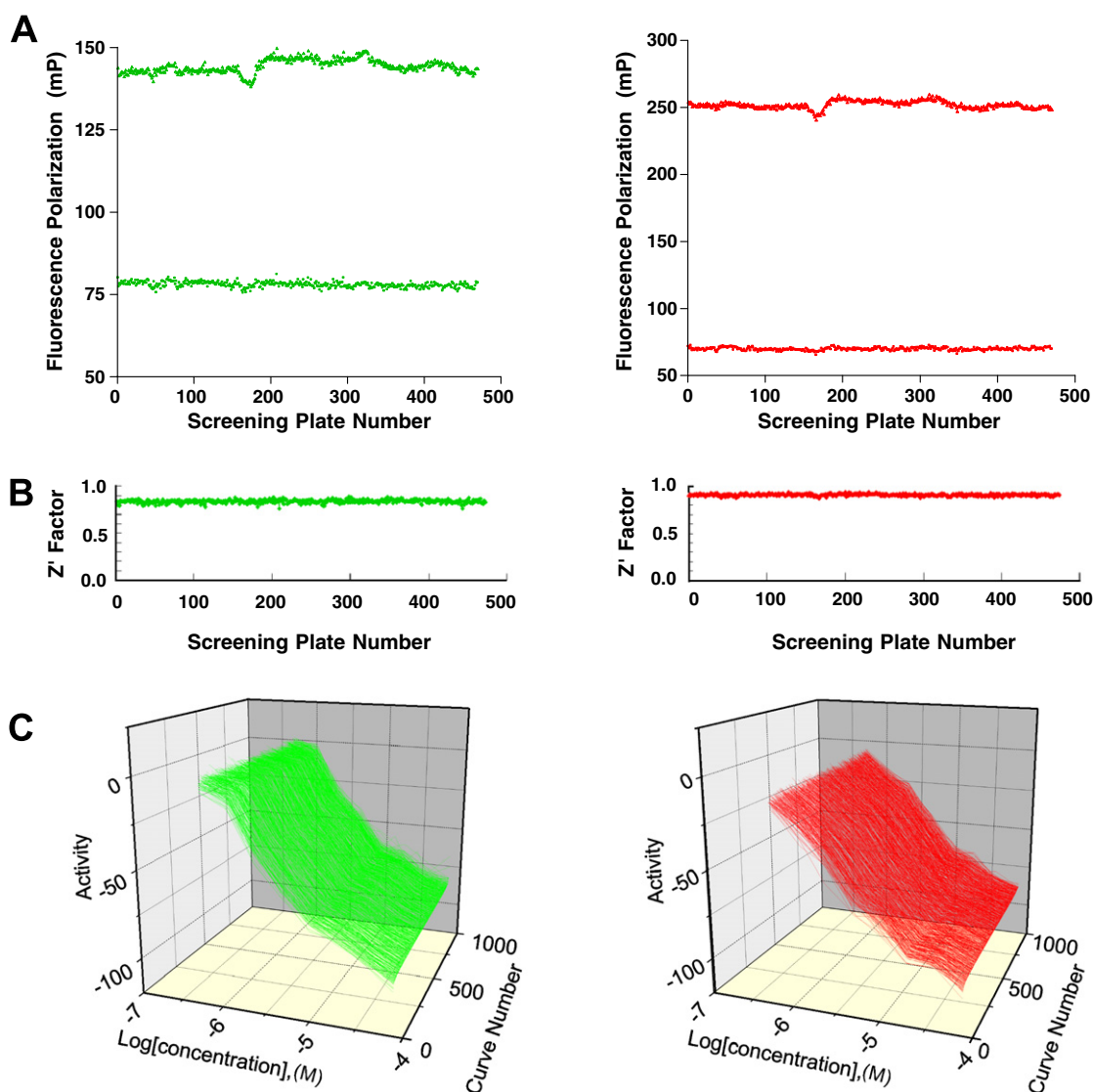


Fig. 3. qHTS performance. Shown are the signal window (A), Z' trend (B), and intraplate control titrations (duplicate curves per plate) (C) as a function of plate number. The plots are color coded to reflect the assay fluorophore.

tion as two batches from different vendors. A number of actives were associated with single-point inhibition at the top concentration, and as such the sigmoidal dose–response curves fitted through the data were of the lowest quality and reproducibility. Table 2 provides a summary of the findings from both screens. The green screen yielded 21 complete curves and 26 single-point top concentration responses, whereas for the red screen the respective counts were 29 and 18. Of the actives exhibiting complete concentration–response curves, 18 were shared between the two

fluorophore assays. Examples of green and red concentration–response curves derived from the primary screen and the follow-up experiments are shown in Fig. 4. We note that although the collected fluorescence intensity data would have allowed us to summarily exclude actives exhibiting autofluorescence, we chose not to do so in this case due to the low number of active samples and the nature of the assay. The overall very low library activity of approximately 0.06% is yet another reflection of the difficulty of finding inhibitors of PPIs.

Table 2
Actives summary by concentration–response curve quality

Fluorophore	Complete curves	Single-point responses	Flat response (inactive)
Green	21	26	75,505
Red	29	18	75,505

Compound follow-up

All 47 samples identified as active in the primary screen were subjected to re-testing by using the same green and red assays. Unlike the interplate (or vertical) titrations employed in the qHTS experiments, the follow-up samples were arrayed in the traditional same-plate fashion [33].

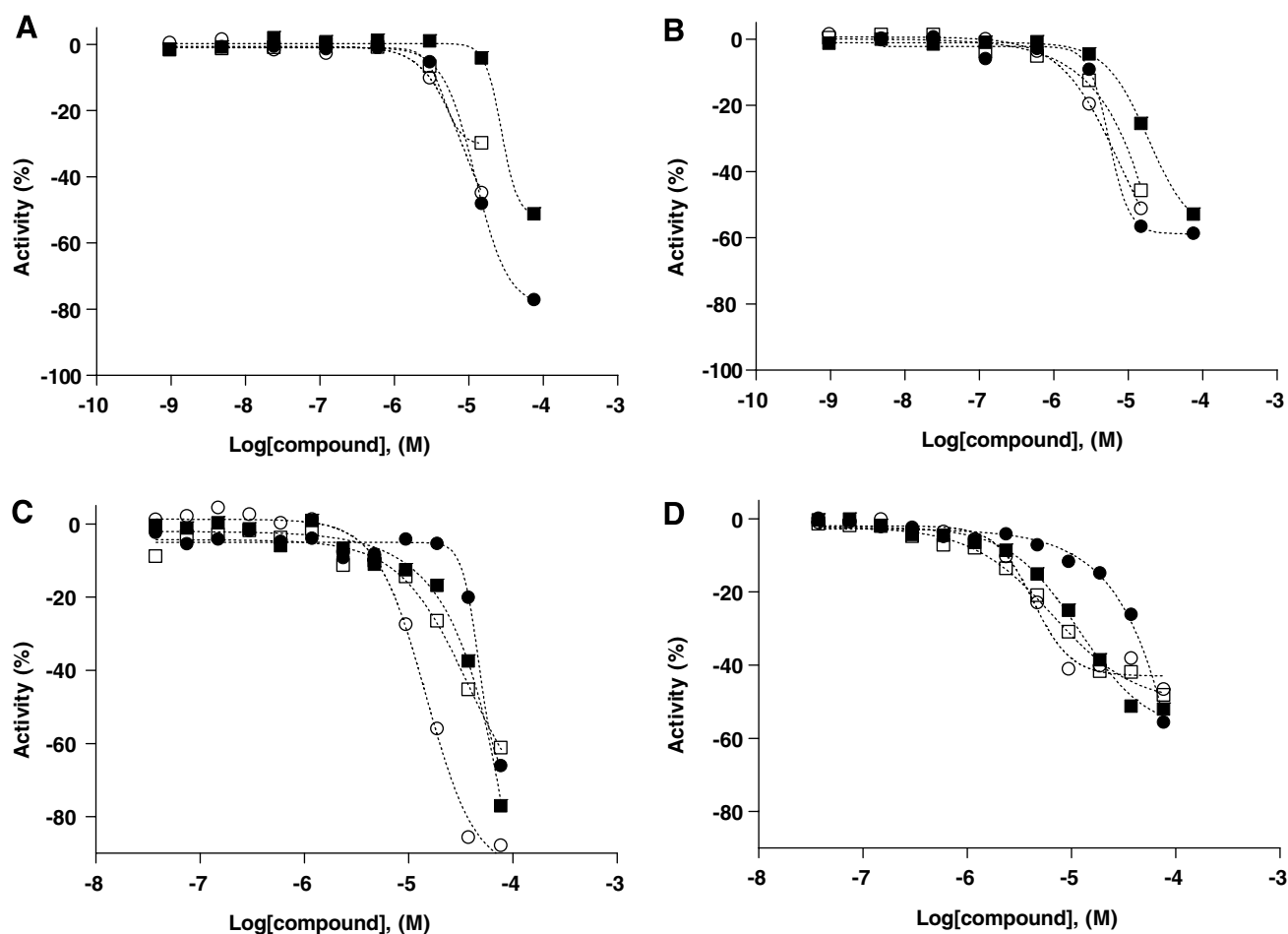


Fig. 4. Examples of concentration–response curves. Shown are curves derived from the primary screen (panel A for green and panel B for red) and the subsequent actives retesting (panel C for green and panel D for red). Compound data refer to NCGC00038539 (●), NCGC00094000 (■), NCGC00097324 (○), and NCGC00097325 (□).

Thus, all 47 samples, occupying one row per sample, were contained within two 1536-well plates. Each sample was tested as 12-point dilution series, developed at twofold steps in duplicate, to yield a total of 24 data points per compound. Unlabeled decapeptide control dilution (12 concentration points in duplicate) was also included in the follow-up tests to ensure the integrity of the interacting BRCT and labeled pBACH1 peptide.

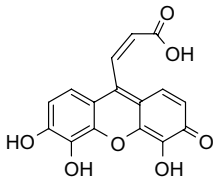
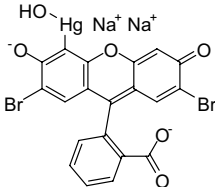
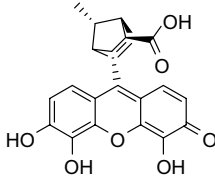
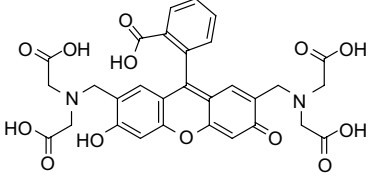
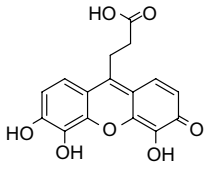
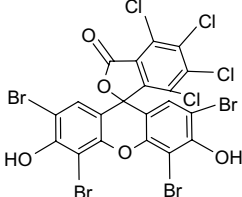
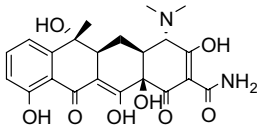
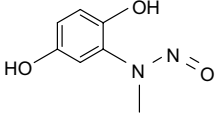
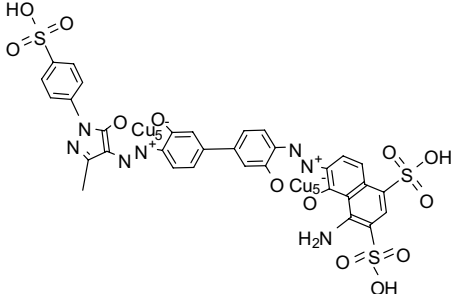
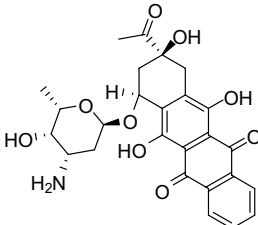
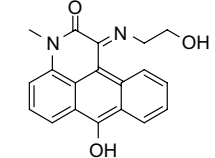
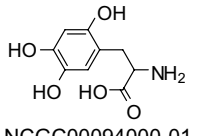
Of the 47 samples retested, 39 showed similar activity in the green assay and 43 reproduced in the red assay as compared with the original screening results. All of the samples that did not reproduce yielded flat concentration–response curves in both colors and were associated with single-point responses in one or both of the primary screens. As such, they had been preflagged as low-confidence actives; therefore, their lack of reproducibility was not unexpected. The structures and activities of compounds that exhibited reproducible effects in both the green and red assays are shown in Table 3. The IC_{50} potencies ranged from single-digit micromolar values (IC_{50} values of 3.2 μ M in the green assay and 7.9 μ M in the red assay for NCGC00094849) to several extrapolated values of more than 100 μ M (with the highest compound concentration tested being 76 μ M).

Although some actives are relatively small in size, we note that the majority of molecules are relatively large with at least one extended ring system. In addition, known bioactive fluorescent molecules and potential quenchers, such as Mercurochrome (NCGC00094822) and Chicago Sky Blue (NCGC00024822), were present among the actives in both colors. Furthermore, one compound showed weak activity ($IC_{50} > 50 \mu$ M) in the green retest assay but was inactive against the red system, and five compounds were weak red active but green inactive. Although such compounds might be true inactives for which the apparent single-color inhibition is a color-associated artifact of quenching or autofluorescence, the converse could be true as well; these compounds might be real actives, but the apparent lack of response in one color might be the result of light attenuation.

Discussion

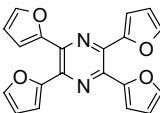
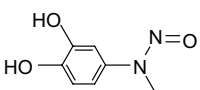
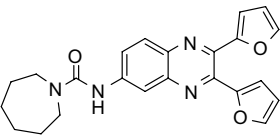
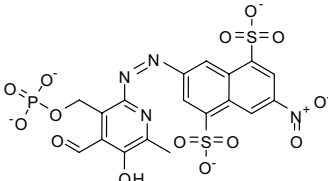
The BRCT–pBACH1 FP assay, previously described and tested in a 384-well format [29], was successfully miniaturized to a 3- μ l volume in a 1536-well plate. A new element to the screening strategy was the development and

Table 3
Structures and follow-up results (IC₅₀ values in μM) of dual-fluorophore active compounds

	Green	Red		Green	Red
	14	6.6		8.5	4.6
NCGC00097323-01			NCGC00094822-01		
	15	4.5		8.5	3.5
NCGC00097324-01			NCGC00094849-01		
	49	6.7		17	3.0
NCGC00097325-01			NCGC00091490-01		
	28	11		128*	44
NCGC00097793-01			NCGC00093830-01		
	66	64		6.1**	11
NCGC00096888-01			NCGC00093976-01		
	87	51		47	38
NCGC00031939-01			NCGC00094000-01		

(continued on next page)

Table 3 (continued)

	Green	Red		Green	Red
	61	70		78	54
NCGC00038539-01			NCGC00094195-01		
	145*	42		136*	15
NCGC00055879-01			NCGC00025105-01		

Note. *, IC_{50} value extrapolated from curve fitting that extends beyond the accuracy of the retest assay that tested the compound at a top concentration of 76 μ M. **Value derived from a validation screen.

implementation of a red-shifted FP assay that employed a TAMRA-labeled peptide of the same sequence. The two-assay, two-probe screening approach served to increase confidence in the actives found. To minimize compound sample variability between the two screen occurrences, we designed and implemented an interleaved assay strategy whereby the green and red screens were performed in one uninterrupted robotic run, with each compound plate being tested against the green and red complexes in immediate succession. The assay interleaving presented here ensured that there were no differences in composition of the compound samples tested between the two assays.

The primary screen against the BCRT–pBACH1 complex was performed in a qHTS format, with every compound tested over a range of concentrations, spanning from tens of micromolar to low nanomolar values, to generate a complete concentration–response profile. Here not only are potencies and efficacies assigned to each active compound, but also false positives and negatives due to outliers associated with individual concentration responses are easily identified in the context of titration, thereby eliminating the need for laborious and infrastructure-intensive cherry-picking, original result replication, and dose–response characterization. Throughout the screen, the interleaved green and red assays performed in a robust manner, yielding Z' values of more than 0.8 that remained flat with the screen progression. The intraplate control titration, which can be viewed as a combined internal standard for both the underlying assay biology and the reproducibility of compound transfer, yielded IC_{50} values that remained within a narrow range throughout the screen (Fig. 3C). The minimum significant ratios (MSRs) were 1.4 for the green screen and 1.2 for the red screen, thereby indicating an overall high level of assay and screening system stability. The MSR screening assay parameter, introduced recently by Eastwood and coworkers [34], serves as

a measure of concentration–response curve reproducibility on repeat testing, and values less than 3 are generally associated with reproducible IC_{50} values. Each library compound was tested at a minimum of seven concentrations, and for each well and fluorophore-type assay three measurements were collected, for a combined total of approximately 4.3 million data points. The reliability and robustness of such screening data sets should make them valuable as depositions in recently established public databases such as PubChem. In addition, the presence of Tween 20 in the assay buffer minimized the interference from promiscuous colloidal aggregators [5].

Autofluorescence from library members is routinely listed as a source of false positives in many assay formats, including FP. Although clever detection schemes, such as obtaining kinetic reaction progress data and performing prereads [3,35,36] as well as profiling the library for fluorescence properties, may allow one to minimize the effect of autofluorescence, or at the very least to grasp its magnitude, there remain instances of genuinely active compounds being fluorescent at the same time. Given this fact and the unique challenges of finding actives in PPI screens, we chose not to discard actives associated with elevated fluorescence intensity values. Indeed, one of our actives, idamycin (also known as idarubicin), has well-documented fluorescent properties [37] while also being known for its antibacterial and antitumor activity.

The total number of actives identified from the dual-fluorophore primary screen was low, and this allowed the retesting and retrospective analysis of essentially all actives without the discrimination against those potentially caused by autofluorescence or quenching and without the application of cutoff filters against single-point responses. The compounds that did confirm were the ones that exhibited complete concentration–response curves from the primary screen, and this further validates the qHTS approach as a

means of identifying reliable actives. The application of both qHTS and dual-color screening assay represents a front loading of sorts and ensures that for a difficult target (e.g., the one under study) combined with a certain assay format, enough measures are taken both to minimize the effect of false positives (thereby avoiding extended, lengthy, and costly cherrypicking) and to maximize the chances of identifying actives. Although orthogonal secondary assays will need to be performed so as to unequivocally establish the biological relevance of the confirmed actives, we note that among the compounds identified here are several that possess attractive features. On the one hand, known bioactives such as idarubicin are well characterized with respect to toxicity and, thus, can be rapidly tested in various in vivo systems. On the other hand, less well-characterized compounds such as NCGC00038539 might serve as starting points for potency optimization.

In summary, the application of a dual-color concentration–response screen against the C-terminal domain of BRCA1 and the phosphorylated peptide portion of the helicase BACH1 allowed fast and reliable identification of actives. The initial characterization of actives by retesting them against both the green and red assays substantiated the majority of activities observed and should serve as a basis for secondary testing of select compounds. More generally, because this work is a result of the NIH Molecular Libraries Initiative created in part to support chemical probe development for novel and poorly characterized targets provided by the academic research community [38], the reported assay and screen strategy and implementation should serve as guidance to researchers seeking to perform HTS on similar targets.

Acknowledgment

This research was supported by the NIH Roadmap for Medical Research and the Intramural Research Program of the National Human Genome Research Institute, National Institutes of Health.

References

- [1] M.R. Arkin, M. Randal, W.L. DeLano, J. Hyde, T.N. Luong, J.D. Oslob, D.R. Raphael, L. Taylor, J. Wang, R.S. McDowell, J.A. Wells, A.C. Braisted, Binding of small molecules to an adaptive protein–protein interface, *Proc. Natl. Acad. Sci. USA* 100 (2003) 1603–1608.
- [2] M.R. Arkin, J.A. Wells, Small-molecule inhibitors of protein–protein interactions: Progressing towards the dream, *Nat. Rev. Drug Disc.* 3 (2004) 301–317.
- [3] J. Inglese, R.L. Johnson, A. Simeonov, M. Xia, W. Zheng, C.P. Austin, D.S. Auld, High-throughput screening assays for the identification of chemical probes, *Nat. Chem. Biol.* 3 (2007) 466.
- [4] B.Y. Feng, A. Shelat, T.N. Doman, R.K. Guy, B.K. Shoichet, High-throughput assays for promiscuous inhibitors, *Nat. Chem. Biol.* 1 (2005) 146–148.
- [5] B.Y. Feng, A. Simeonov, A. Jadhav, K. Babaoglu, J. Inglese, B.K. Shoichet, C.P. Austin, A high-throughput screen for aggregation-based inhibition in a large compound library, *J. Med. Chem.* 50 (2007) 2385–2390.
- [6] A.A. Bogan, K.S. Thorn, Anatomy of hot spots in protein interfaces, *J. Mol. Biol.* 280 (1998) 1–9.
- [7] J.J. Tesmer, Pharmacology: Hitting the hot spots of cell signaling cascades [comment], *Science* 312 (2006) 377–378.
- [8] S.B. Cantor, D.W. Bell, S. Ganesan, E.M. Kass, R. Drapkin, S. Grossman, D.C. Wahrer, D.C. Sgroi, W.S. Lane, D.A. Haber, D.M. Livingston, BACH1, a novel helicase-like protein, interacts directly with BRCA1 and contributes to its DNA repair function, *Cell* 105 (2001) 149–160.
- [9] H. Kim, J. Huang, J. Chen, CCDC98 is a BRCA1–BRCT domain-binding protein involved in the DNA damage response, *Nat. Struct. Mol. Biol.* 14 (2007) 710–715.
- [10] B. Wang, S. Matsuoka, B.A. Ballif, D. Zhang, A. Smogorzewska, S.P. Gygi, S.J. Elledge, Abraxas and RAP80 form a BRCA1 protein complex required for the DNA damage response, *Science* 316 (2007) 1194–1198.
- [11] X. Yu, L.C. Wu, A.M. Bowcock, A. Aronheim, R. Baer, The C-terminal (BRCT) domains of BRCA1 interact in vivo with CtIP, a protein implicated in the CtBP pathway of transcriptional repression, *J. Biol. Chem.* 273 (1998) 25388–25392.
- [12] I.A. Manke, D.M. Lowery, A. Nguyen, M.B. Yaffe, BRCT repeats as phosphopeptide-binding modules involved in protein targeting, *Science* 302 (2003) 636–639.
- [13] X. Yu, J. Chen, DNA damage-induced cell cycle checkpoint control requires CtIP, a phosphorylation-dependent binding partner of BRCA1 C-terminal domains, *Mol. Cell. Biol.* 24 (2004) 9478–9486.
- [14] X. Yu, C.C. Chini, M. He, G. Mer, J. Chen, The BRCT domain is a phospho-protein binding domain, *Science* 302 (2003) 639–642.
- [15] Z. Liu, J. Wu, X. Yu, CCDC98 targets BRCA1 to DNA damage sites, *Nat. Struct. Mol. Biol.* 14 (2007) 716–720.
- [16] H. Kim, J. Chen, X. Yu, Ubiquitin-binding protein RAP80 mediates BRCA1-dependent DNA damage response, *Science* 316 (2007) 1202–1205.
- [17] B. Sobhian, G. Shao, D.R. Lilli, A. Culhane, L.A. Moreau, B. Xia, D.M. Livingston, R.A. Greenberg, RAP80 targets BRCA1 to specific ubiquitin structures at DNA damage sites, *Science* 316 (2007) 1198–1202.
- [18] G.L. Lokesh, B.K. Muralidhara, S.S. Negi, A. Natarajan, Thermodynamics of phosphopeptide tethering to BRCT: The structural minima for inhibitor design, *J. Am. Chem. Soc.* 129 (2007) 10658–10659.
- [19] A.K. Varma, R.S. Brown, G. Birrane, J.A. Ladias, Structural basis for cell cycle checkpoint control by the BRCA1–CtIP complex, *Biochemistry* 44 (2005) 10941–10946.
- [20] R.S. Williams, M.S. Lee, D.D. Hau, J.N. Glover, Structural basis of phosphopeptide recognition by the BRCT domain of BRCA1, *Nat. Struct. Mol. Biol.* 11 (2004) 519–525.
- [21] M.V. Botuyan, Y. Nomine, X. Yu, N. Juranic, S. Macura, J. Chen, G. Mer, Structural basis of BACH1 phosphopeptide recognition by BRCA1 tandem BRCT domains, *Structure* 12 (2004) 1137–1146.
- [22] J.A. Clapperton, I.A. Manke, D.M. Lowery, T. Ho, L.F. Haire, M.B. Yaffe, S.J. Smerdon, Structure and mechanism of BRCA1 BRCT domain recognition of phosphorylated BACH1 with implications for cancer, *Nat. Struct. Mol. Biol.* 11 (2004) 512–518.
- [23] E.N. Shiozaki, L. Gu, N. Yan, Y. Shi, Structure of the BRCT repeats of BRCA1 bound to a BACH1 phosphopeptide: Implications for signaling, *Mol. Cell* 14 (2004) 405–412.
- [24] M. Rodriguez, X. Yu, J. Chen, Z. Songyang, Phosphopeptide binding specificities of BRCA1 COOH-terminal (BRCT) domains, *J. Biol. Chem.* 278 (2003) 52914–52918.
- [25] J. Inglese, D.S. Auld, A. Jadhav, R.L. Johnson, A. Simeonov, A. Yasgar, W. Zheng, C.P. Austin, Quantitative high-throughput screening: A titration-based approach that efficiently identifies biological activities in large chemical libraries, *Proc. Natl. Acad. Sci. USA* 103 (2006) 11473–11478.
- [26] P.H. Cleveland, P.J. Koutz, Nanoliter dispensing for uHTS using pin tools, *Assay Drug Dev. Technol.* 3 (2005) 213–225.

- [27] A.V. Hill, The possible effects of the aggregation of the molecule of haemoglobin on its dissociation curves, *J. Physiol. (Lond.)* 40 (1910) 4–7.
- [28] W.D. Niles, P.J. Coassin, Piezo- and solenoid valve-based liquid dispensing for miniaturized assays, *Assay Drug Dev. Technol.* 3 (2005) 189–202.
- [29] G.L. Lokesh, A. Rachamalla, G.D. Kumar, A. Natarajan, High-throughput fluorescence polarization assay to identify small molecule inhibitors of BRCT domains of breast cancer gene 1, *Anal. Biochem.* 352 (2006) 135–141.
- [30] X. Cheng, J. Hochlowski, H. Tang, D. Hepp, C. Beckner, S. Kantor, R. Schmitt, Studies on repository compound stability in DMSO under various conditions, *J. Biomol. Screen.* 8 (2003) 292–304.
- [31] B.A. Kozikowski, T.M. Burt, D.A. Tirey, L.E. Williams, B.R. Kuzmak, D.T. Stanton, K.L. Morand, S.L. Nelson, The effect of room-temperature storage on the stability of compounds in DMSO, *J. Biomol. Screen.* 8 (2003) 205–219.
- [32] J.H. Zhang, T.D. Chung, K.R. Oldenburg, A simple statistical parameter for use in evaluation and validation of high throughput screening assays, *J. Biomol. Screen.* 4 (1999) 67–73.
- [33] A. Yasgar, P. Shinn, S. Michael, W. Zheng, A. Jadhav, D. Auld, C. Austin, J. Inglese, A. Simeonov, Compound management for quantitative high-throughput screening, *J. Assoc. Lab. Automat.* (in press).
- [34] B.J. Eastwood, M.W. Farnen, P.W. Iversen, T.J. Craft, J.K. Smallwood, K.E. Garbison, N.W. Delapp, G.F. Smith, The minimum significant ratio: A statistical parameter to characterize the reproducibility of potency estimates from concentration–response assays and estimation by replicate experiment studies, *J. Biomol. Screen.* 11 (2006) 253–261.
- [35] A. Simeonov, A. Jadhav, A. Sayed, Y. Wang, M. Nelson, C. Thomas, J. Inglese, D. Williams, C. Austin, Quantitative high-throughput screen identifies inhibitors of the *Schistosoma mansoni* redox cascade, *PLoS Neglected Trop. Dis.* 2 (2008) e127.
- [36] E.L. White, K. Southworth, L. Ross, S. Cooley, R.B. Gill, M.I. Sosa, A. Manoukhova, L. Rasmussen, C. Goulding, D. Eisenberg, T.M. Fletcher III, A novel inhibitor of *Mycobacterium tuberculosis* pantothenate synthetase, *J. Biomol. Screen.* 12 (2007) 100–105.
- [37] T. Perez-Ruiz, C. Martinez-Lozano, A. Sanz, E. Bravo, Simultaneous determination of doxorubicin, daunorubicin, and idarubicin by capillary electrophoresis with laser-induced fluorescence detection, *Electrophoresis* 22 (2001) 134–138.
- [38] C.P. Austin, L.S. Brady, T.R. Insel, F.S. Collins, NIH Molecular Libraries Initiative, *Science* 306 (2004) 1138–1139.